Electronic Structure Analysis of Interface between Support Surface and Cocatalyst for Water Splitting Layer Photocatalyst by DFT Method

Yoshiki Shimodaira,[1] Akihiko Kudo,[1,2] and Hisayoshi Kobayashi*[3]
[1]*Department of Applied Chemistry, Faculty of Science, Tokyo University of Science, 1-3 Kagurazaka, Shinjuku-ku, Tokyo 162-8601*
[2]*Core Research for Evolutional Science and Technology, Japan Science and Technology Agency (CREST, JST)*
[3]*Department of Chemistry and Materials Technology, Kyoto Institute of Technology, Matsugasaki, Sakyo-ku, Kyoto 606-8585*

(Received October 10, 2006; CL-061188; E-mail: kobayashi@chem.kit.ac.jp)

The electronic structures of cocatalyst/photocatalyst interface ($NiO_x/K_2La_2Ti_3O_{10}$) used for water splitting were investigated by the two-dimentional surface model DFT calculations. The difference in electronic states at the interface between the cocatalyst and photocatalyst was characterized in terms of the crystal faces of support photocatalyst. This result explains the difference in mobility of the photoexcited electron from the support photocatalyst to the cocatalyst between two different crystal surfaces of photocatalyst.

It has been common strategy that the electronic states of the water splitting photocatalyst materials are discussed from a quantum chemistry viewpoint.[1–3] Usually the bulk structures are employed for the calculation with the plane wave based density functional theory method. These results bring about the knowledge for the development of new photocatalytic materials. However, computational chemistry approach has not yet been done to clarify the electron structure of the interface between cocatalyst and support photocatalyst although it is the most interesting for the photocatalytic reaction. In recent years, the quantum chemistry methodology for vacuum slab has been developed.[4] Consequently, the techniques managing the crystal surface and interface structures as the two-dimensional periodic boundary condition model and with a high degree of accuracy have been established and incorporated in many MD and DFT method programs. It means that the theoretical approaches to the difficult region from the experimental analysis become possible. In this study, we try to analyze to the electronic structure at the interfaces of two different crystal surface of photocatalyst based on the DFT calculations. As the calculation models of cocatalyst/photocatalyst, $NiO_x/K_2La_2Ti_3O_{10}$ photocatalyst[5,6] for water splitting was adopted in this letter, for which much information such as crystal structure, surface physical properties, cocatalyst condition, and photocatalytic properties is available. It has been already reported that the inside of NiO_x particle is Ni metal whereas the surface is NiO oxide.[7,8] Ni metal is in contact with the support surface of $K_2La_2Ti_3O_{10}$ photocatalyst.

For selection of the loading surface, the (002) and (101) crystal surfaces of $K_2La_2Ti_3O_{10}$ photocatalyst were selected by the morphology analysis using molecular dynamics[9,10] and the experimental reports.[5,6] The two interface unit cell models consisting of the (002) and (101) surfaces of the photocatalyst having six atom layers and the Ni(111) cocatalyst having four atom layers were created. For the photocatalyst side, the most stable surface is a polar face consisted of O atoms. However, the (101) crystal surfaces of $K_2La_2Ti_3O_{10}$ contained unsaturated Ti site partially. The optimized structure is shown in Figure 1. The thickness of vacuum region was set to ca. 20 Å. The band calculation for these interface models was carried out using the plane wave DFT program package Castep.[11] The Perdew–Burke–Ernzerhof functional was employed.[12] The ultrasoft core potential scheme was employed.[13] The valence electronic configurations for individual atoms were $3d^84s^2$ for Ni, $3s^23p^64s^1$ for K, $5s^25p^65d^16s^2$ for La, $3s^23p^63d^24s^2$ for Ti, and $2s^22p^4$ for O. The kinetic energy cutoff was set to 300 eV.

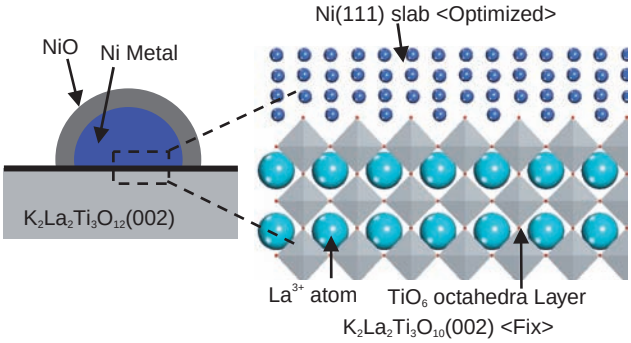

Figure 1. $Ni(111)/K_2La_2Ti_3O_{10}(002)$ surface unit cell models.

For both the $Ni(111)/K_2La_2Ti_3O_{10}(002)$ and (101) interface models, it was revealed that the band gap region of the $K_2La_2Ti_3O_{10}$ photocatalyst was energetically overlapped with the Ni3d bands. Additionally, the Fermi level of Ni metal appeared in the band gap region and one third of the band gap width below the bottom of conduction band. Figure 2 shows the electron density contour maps for the bottom of conduction

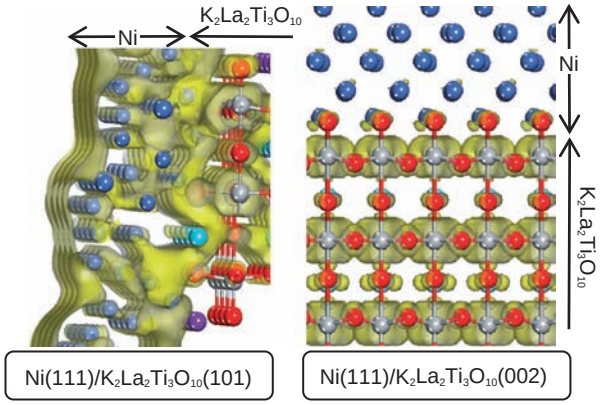

Figure 2. Electron density contour maps for the bottom of conduction band of $K_2La_2Ti_3O_{10}$ photocatalyst.

Copyright © 2007 The Chemical Society of Japan

Table 1. Calculation results of interface unit cell models

	Ni(111) /$K_2La_2Ti_3O_{10}$(101)	Ni(111) /$K_2La_2Ti_3O_{10}$(002)
Ni–Ni Bonding strength (Mulliken bond population)	0.90–1.10	0.90–1.10
Charge polarization in Ni metal (Mulliken charge population)	Whole: +0.05	Outer: +0.26 Inner: −0.05
Semiquantitative work function of Ni(111)[a] (Calc.) (eV)	ca. 2.8	ca. 3.3

[a]Work function of bulk Ni(111) (Expt.[14]): 5.35 eV.

band of $K_2La_2Ti_3O_{10}$ photocatalyst. In the Ni(111)/$K_2La_2Ti_3O_{10}$(101) interface model, the Ni3d+Ti3d hybrid orbitals spread from the interface region to the Ni bulk. On the other hand, for the Ni(111)/$K_2La_2Ti_3O_{10}$(002) interface model, the electron density is only localized within the photocatalyst. It suggests that the photoexcited electron transfer to Ni cocatalyst is more smooth for the (101) crystal face of $K_2La_2Ti_3O_{10}$ than the (002) crystal face.

The Mulliken population analysis was carried out to estimate the bonding nature and charge on atoms.[15,16] In both the interface models, the values of Ni–Ni bonding strength were equal as shown in Table 1. However, the polarization of charge was recognized between the outer and inner Ni atoms within the Ni(111) slab attached on $K_2La_2Ti_3O_{10}$(002) model. This means that the electron mobility to Ni bulk via the $K_2La_2Ti_3O_{10}$(002) interface is constrained, although Ni metal bulk has generally high conductivity. Therefore, it is concluded that the performance of the interfacial electron transfer differs for each crystal faces of $K_2La_2Ti_3O_{10}$ photocatalyst.

Moreover, the semiquantitative work function (WF_{cal}) of nickel metal bulk was calculated using the electrostatic potential (V_{pot}) of the vacuum slab and the relative Fermi level (E_{Fermi}) decided by the electron occupation, as in eq 1.[4]

$$WF_{cal} = (-V_{pot}) - E_{Fermi} \quad (1)$$

The semiquantitative work function is a relative value, and it can not be compared with the experimental values. It is possible to compare with two values of WF_{cal} as the Ni level position of cocatalyst in each Ni(111)/$K_2La_2Ti_3O_{10}$ unit cell model. According to the calculation results, the value of WF_{cal} of Ni(111)/$K_2La_2Ti_3O_{10}$(101) model was smaller than that of Ni(111)/$K_2La_2Ti_3O_{10}$(002) model, and then the photoexcited electron which transferred to Ni metal cocatalyst from (101) crystal face can keep up high potential. It means that the keeping of high potential leads to the good driving force for the H^+ reduction. Therefore, it is concluded that the position of Ni3d level is influenced by the crystal face of the $K_2La_2Ti_3O_{10}$ photocatalyst and brings to the difference in the efficiency of photocatalytic activity for H_2 evolution as shown in Figure 3.

From the viewpoint of both the mobility of the electron transfer on the interface and the work function of Ni metal, it is concluded that the loading on (101) crystal face is favorable. It is the first time to our knowledge that the electronic structures of the interface region between the cocatalyst and each crystal faces of photocatalyst can be characterized by the surface model DFT calculations with the two-dimentional periodic boundary condition. Although the traditional cocatalyst loading was carried out on all crystal faces, this study suggests a possibility that

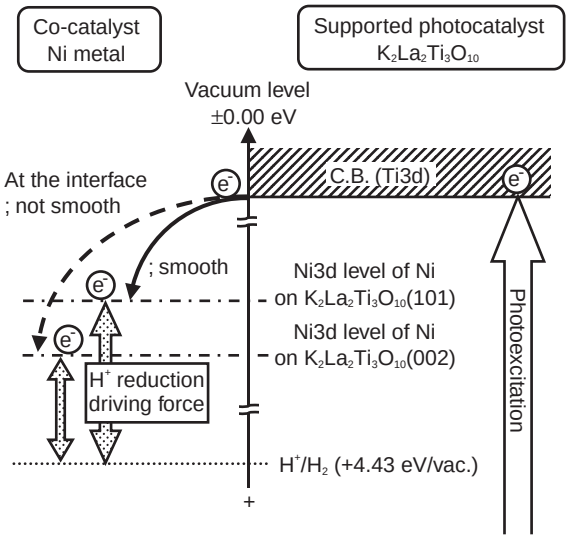

Figure 3. Route of photoexcited electron transfer.

improvement of photocatalytic activity will be attained by the selective loading on the crystal faces through good electron mobility and the selective crystal growth exposing favorable crystal faces. The present calculation technique is also applicable for other cocatalyst/photocatalyst systems.

This work was supported by Core Research for Evolutional Science and Technology (CREST) of the Japan Science and Technology Agency (JST), a Grant-in-Aid (No. 14050090) for the Priority Area Research (No. 417) from the Ministry of Education, Culture, Sports, Science and Technology.

References

1 H. Kato, H. Kobayashi, A. Kudo, *J. Phys. Chem. B* **2002**, *106*, 12441.
2 J. Sato, N. Saito, Y. Yamada, K. Maeda, T. Takata, J. N. Kondo, M. Hara, H. Kobayashi, K. Domen, Y. Inoue, *J. Am. Chem. Soc.* **2005**, *127*, 4150.
3 Y. Shimodaira, H. Kato, H. Kobayashi, A. Kudo, *J. Phys. Chem. B* **2006**, *110*, 17790.
4 A. Seidl, A. Gorling, P. Vogl, J. A. Majewski, M. Levy, *Phys. Rev. B* **1996**, *53*, 3764.
5 T. Takata, K. Shinohara, A. Tanaka, M. Hara, J. N. Kondo, K. Domen, *J. Photochem. Photobiol., A* **1997**, *106*, 45.
6 T. Takata, Y. Furumi, K. Shinohara, A. Tanaka, M. Hara, J. N. Kondo, K. Domen, *Chem. Mater.* **1997**, *9*, 1063.
7 K. Domen, A. Kudo, T. Onishi, *J. Catal.* **1986**, *102*, 92.
8 K. Domen, A. Kudo, T. Onishi, N. Kosugi, H. Kuroda, *J. Phys. Chem.* **1986**, *90*, 292.
9 G. Z. Wulff, *Krystallogr.* **1901**, *34*, 449.
10 P. Bennema, *J. Cryst. Growth* **1996**, *166*, 17.
11 M. C. Payne, M. P. Teter, D. C. Allan, T. A. Arias, *Rev. Mod. Phys.* **1992**, *64*, 1045.
12 J. P. Perdew, K. Burke, M. Ernzerhof, *Phys. Rev. Lett.* **1996**, *77*, 3865.
13 D. Vanderbilt, *Phys. Rev. B* **1990**, *41*, 7892.
14 *CRC Handbook of Chemistry and Physics*, 66th ed.
15 R. S. Mulliken, *J. Chem. Phys.* **1955**, *23*, 1833.
16 E. R. Davidson, S. Chakravorty, *Theor. Chim. Acta* **1992**, *83*, 319.

Published on the web (Advance View) December 16, 2006; doi:10.1246/cl.2007.170